Multifractal Bernoulli fluctuations in disordered mesoscopic systems

1998 J. Phys. A: Math. Gen. 31 L707

(http://iopscience.iop.org/0305-4470/31/41/001)

J. Phys. A: Math. Gen. **31** (1998) L707–L711. Printed in the UK PII: S0305-4470(98)93291-7

LETTER TO THE EDITOR

Multifractal Bernoulli fluctuations in disordered mesoscopic systems

A Bershadskii
PO Box 39953, Ramat-Aviv 61398, Tel-Aviv, Israel

Received 14 April 1998

Abstract. It is shown that multifractal Bernoulli fluctuations appear at morphological phase transition from monofractality to multifractality. This type of fluctuation is studied in detail and it is shown that the multifractal fluctuations of wavefunctions at disorder-induced localization–delocalization transitions can be identified as multifractal Bernoulli fluctuations (both in two- and three-dimensional cases).

Disorder-induced localization–delocalization transitions are characterized by multifractal fluctuations of the wavefunctions on all length scales up to system size L (see, for instance, [1–9] and references therein). The multifractal fluctuations lead to anomalous behaviour of the transport properties [1–11]. Thus, to understand the statistical nature of these fluctuations is a real problem.

(1) A continuous set of the exponents, so-called generalized dimensions (D_q) is usually used to described the multifractal behaviour. These generalized dimensions are determined from equation

$$Z(q) = \sum_{i=1}^{N} [\mu_i(r)]^q \sim (r/L)^{\tau(q)} \tag{1}$$

where

$$\tau(q) = (q-1)D_q \tag{2}$$

and the lattice with linear system size L is partitioned into N boxes of size r ($N \sim (L/r)^d$ and d is the topological dimension of the lattice). The measure μ_i is the amplitude of the wavefunction squared on the ith box and the limit $r/L \to 0$ is taken.

Let us define

$$\overline{\mu_i} = \mu_i / \max_i\{\mu_i\}. \tag{3}$$

Then

$$\langle \overline{\mu}^p \rangle = \frac{1}{N} \sum_i \overline{\mu_i}^p. \tag{4}$$

The simplest structure that can be used for fractal description is a system for which $\overline{\mu_i}$ can take only two values 0 and 1. It follows from (3) and (4) that for such a system (with $q > 0$)

$$\langle \overline{\mu}^p \rangle = \langle \overline{\mu} \rangle \tag{5}$$

0305-4470/98/410707+05$19.50

and fluctuations in this system can be identified as Bernoulli fluctuations [12]. It is clear that the Bernoulli fluctuations can be *monofractal* only.

Generalization of (5) in the form of a generalized scaling

$$\langle \overline{\mu}^p \rangle \sim \langle \overline{\mu} \rangle^{f(p)} \tag{6}$$

can be used to describe more complex (multifractal) systems. We use invariance of the generalized scaling (6) with dimension transform [13]

$$\overline{\mu_i} \to \overline{\mu_i}^{\lambda} \tag{7}$$

to find $f(p)$. This invariance means that

$$\langle (\overline{\mu}^{\lambda})^p \rangle \sim \langle (\overline{\mu}^{\lambda}) \rangle^{f(p)} \tag{8}$$

for all positive λ. Then, it follows from (6) and (8) that

$$\langle (\overline{\mu})^{\lambda p} \rangle \sim \langle \overline{\mu} \rangle^{f(\lambda p)} \sim \langle \overline{\mu} \rangle^{f(\lambda) f(p)}. \tag{9}$$

Hence,

$$f(\lambda p) = f(\lambda) f(p). \tag{10}$$

The general solution of functional equation (10) is

$$f(p) = p^{\gamma} \tag{11}$$

where γ is a positive number (cf [14]). It should be noted that the case $\gamma = 1$ corresponds to Gaussian fluctuations [15]. We, however, shall consider the limit $\gamma \to 0$ (i.e. transition to the Bernoulli fluctuations). This transition is non-trivial. Indeed, let us consider generalized scaling

$$F_{qm} \sim F_{km}^{\alpha(q,k,m)} \tag{12}$$

where

$$F_{qm} = \langle \overline{\mu}^q \rangle / \langle \overline{\mu}^m \rangle. \tag{13}$$

Substituting (6) into (12), (13) and using (11) we obtain

$$\alpha(q, k, m) = \frac{q^{\gamma} - m^{\gamma}}{k^{\gamma} - m^{\gamma}}.$$

Hence,

$$\lim_{\gamma \to 0} \alpha(q, k, m) = \frac{\ln(q/m)}{\ln(k/m)}. \tag{14}$$

If there is ordinary scaling

$$\langle \overline{\mu}^p \rangle \sim (r/L)^{\zeta_p} \tag{15}$$

then

$$\alpha(q, k, m) = \frac{\zeta_q - \zeta_m}{\zeta_k - \zeta_m}. \tag{16}$$

From comparison of (14) and (16) we obtain at the limit $\gamma \to 0$

$$\frac{\zeta_q - \zeta_m}{\zeta_k - \zeta_m} = \frac{\ln(q/m)}{\ln(k/m)}. \tag{17}$$

The general solution of functional equation (17) is

$$\zeta_q = a + c \ln q \tag{18}$$

where a and c are constants.

If we use the relationship

$$\max_i\{\mu_i\} \sim (r/L)^{D_\infty} \tag{19}$$

(see, for instance, [16]), then it follows from (2), (3) and (15), (18), (19) that

$$D_q = D_\infty + c\frac{\ln q}{(q-1)} \tag{20}$$

for the multifractal Bernoulli fluctuations (i.e. the fluctuations which appear at the limit $\gamma \to 0$).

(2) From (6), (15) and (18) we can find $f(p)$ corresponding to the multifractal Bernoulli fluctuations

$$f(p) = 1 + \frac{c}{a}\ln p \tag{21}$$

where $a = d - D_\infty$. One can see that for finite c the dimension-invariance is broken at the limit $\gamma \to 0$.

Let us find the characteristic function of the multifractal Bernoulli distribution. It is known that the characteristic function $\chi(\lambda)$ can be represented by the following series (see, for instance [12]):

$$\chi(\lambda) = \sum_{p=0}^{\infty}\frac{(\mathrm{i}\lambda)^p}{p!}\langle\overline{\mu}^p\rangle. \tag{22}$$

Then using (6) and (21) we obtain from (22)

$$\chi(\lambda) = 1 + \langle\overline{\mu}\rangle\sum_{p=1}^{\infty}\frac{(\mathrm{i}\lambda)^p}{p!}p^\beta \tag{23}$$

where

$$\beta = \frac{c}{(d - D_\infty)}\ln\langle\overline{\mu}\rangle. \tag{24}$$

The characteristic function (23) gives a complete description of the multifractal Bernoulli distribution.

(3) In a recent paper [9] numerical calculations of the local density states at disorder-induced localization–delocalization transitions were performed for two- and three-dimensional network models of the integer quantum Hall effect [4] and the so-called quantum Hall insulator, respectively. Figure 1 (adapted from [9]) shows the function $D_q/2$ calculated for a two-dimensional network model at the quantum Hall critical point [4, 8]. In this figure the axes are chosen for comparison between the data (dots) and the multifractal Bernoulli representation (20) (straight line). One can see good agreement between the data and the representation (20). Figure 2 (also adapted from [9]) shows the analogous data calculated in [9] for a three-dimensional network [10]. In contrast to the two-dimensional network, here a band of extended states appears. And again, the multifractal Bernoulli fluctuations appear at the mobility edge of this system, as one can see from figure 2 (the straight line corresponds to the multifractal Bernoulli representation (20)). Schreiber and Grussbach [6] have examined the three-dimensional Schrödinger equation with a random potential at each lattice site, described by the Anderson Hamiltonian:

$$H = \sum_{\boldsymbol{x}}\varepsilon_{\boldsymbol{x}}|\boldsymbol{x}\rangle\langle\boldsymbol{x}| + V\sum_{(\boldsymbol{x},\boldsymbol{y})}|\boldsymbol{x}\rangle\langle\boldsymbol{y}| \tag{25}$$

with constant nearest-neighbour transfer integral V and random potential $\varepsilon_{\boldsymbol{x}}$ governed by a uniform distribution of width W. The sums extend over all lattice sites $\boldsymbol{x}$, and $(\boldsymbol{x}, \boldsymbol{y})$

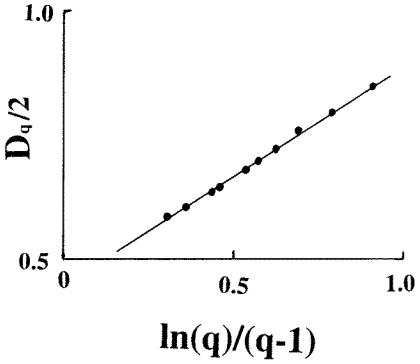

Figure 1. Generalized dimensions $D_q/2$ against $\ln(q)/(q-1)$ for a two-dimensional network model at the quantum Hall critical point. Data (dots) taken from [9]. The straight line is drawn for comparison with representation (20).

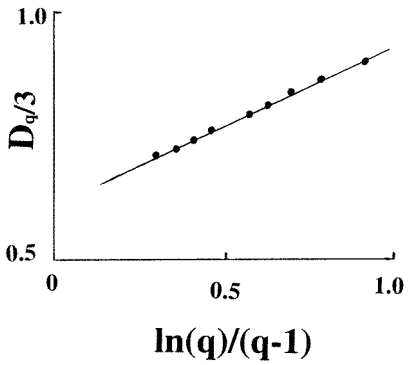

Figure 2. Generalized dimensions $D_q/3$ against $\ln(q)/(q-1)$ for a three-dimensional network model. Data (dots) taken from [9]. The straight line is drawn for comparison with representation (20).

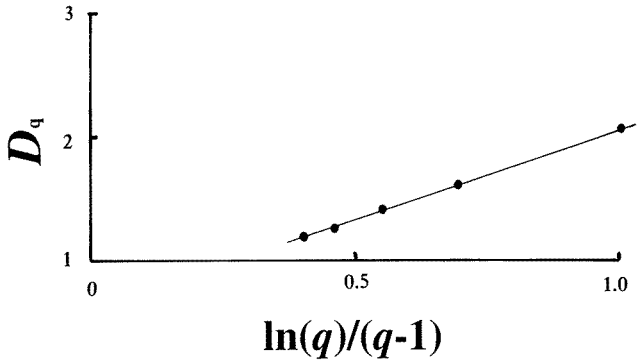

Figure 3. Generalized dimensions D_q against $\ln(q)/(q-1)$ for three-dimensional Anderson transition. Data (dots) taken from [6]. The straight line is drawn for comparison with representation (20).

denotes all nearest-neighbour pairs of sites in a three-dimensional lattice. The parameter W describes the strength disorder and the metallic–insulator transition is believed to occur at $W_c \simeq 16.5$ for three-dimensional samples [17, 18]. For $W > W_c$ all states are localized and the conductivity is zero, while for $W < W_c$ mobility edges appear in the band separating localized states near the band centre. In [6] the model equation was numerically studied at the critical region and the generalized dimensions D_q were calculated by plotting $\ln(\langle \sum_x |\psi_n(x)|^{2q} \rangle)$ against $\ln(L)$. These data (taken from [6]) are shown in figure 3. The axes on this figure are chosen for comparison with representation (20) (straight line). One can see good agreement between the data (dots) and this representation. In [7] an analogous multifractal spectrum was calculated for eigenstates in the critical regime of a two-dimensional electron gas in high magnetic field. Figure 4 (adapted from [7]) shows these data. One can see good agreement between the data (dots) and the Bernoulli representation (20).

(4) It has been shown that the multifractal Bernoulli fluctuations appear at the morphological phase transition from monofractality to multifractality and therefore

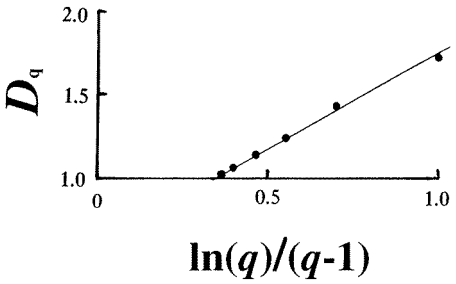

Figure 4. Generalized dimensions D_q against $\ln(q)/(q-1)$ for multifractal wavefunctions in the critical regime of two-dimensional disordered electron systems in high magnetic field. Data (dots) taken from [7]. The straight line is drawn for comparison with representation (20).

appearance of these fluctuations at the disorder-induced localized–delocalized transitions is evidence of the morphological nature of this phenomenon. Moreover, the multifractal Bernoulli representation (20) gives complete description of the multifractal properties of the wavefunctions for $q > 1$ only (i.e. for intensive fluctuations). It can be related to the normalization (3) [16]. Using Hölder inequality it can also be shown [16] that the weak fluctuations (i.e. for $q < 1$) cannot be pure Bernoulli ones in this case. It means, in particular, that the morphological phase transition from monofractality to multifractality should not lead to singular behaviour of the function D_q (or its derivatives) on the real q-axis. [16].

The author is grateful to D Stauffer for discussions and to the Machanaim Center (Jerusalem) for support.

References

[1] Aoki H 1983 *J. Phys. C: Solid State Phys.* **16** L205
[2] Schreiber M 1985 *Phys. Rev.* B **31** 6146
[3] Aoki H 1986 *Phys. Rev.* B **33** 7310
[4] Chalker J T and Coddington P D 1988 *J. Phys. C: Solid State Phys.* **21** 2665
[5] Ono Y, Ohtsuki T and Kramer B 1989 *J. Phys. Soc. Japan* **58** 1705
[6] Schreiber M and Grussbach H 1991 *Phys. Rev. Lett.* **67** 607
[7] Pook W and Janssen M 1991 *Z. Phys.* B **82** 295
[8] Klesse R and Metzler M 1995 *Europhys. Lett.* **32** 229
[9] Huckestein B and Klesse R 1997 *Phys. Rev.* B **55** R7303
[10] Chalker J T and Dohmen A 1995 *Phys. Rev. Lett.* **75** 4496
[11] Huckenstein B and Schweitzer L 1994 *Phys. Rev. Lett.* **72** 713
[12] Parzen E 1967 *Modern Probability Theory and Its Applications* (New York: Wiley) section 3
[13] Bershadskii A 1997 *Europhys. Lett.* **39** 587
[14] Havlin S and Bunde A 1989 *Physica* **38D** 184
[15] Beck J and Chen W W L 1987 *Irregularities of Distribution* (Cambridge: Cambridge University Press) section 1
[16] Bershadskii A and Tsinober A 1992 *Phys. Lett.* A **165** 37
[17] Bulka B, Schreiber M and Kramer B 1987 *Z. Phys.* B **66** 21
[18] Shklovskii B I *et al* 1993 *Phys. Rev.* B **47** 11 487